THE JOURNAL OF BIOLOGICAL CHEMISTRY VOL. 286, NO. 7, pp. 5846–5854, February 18, 2011
Printed in the U.S.A.

Dopamine D_1-histamine H_3 Receptor Heteromers Provide a Selective Link to MAPK Signaling in GABAergic Neurons of the Direct Striatal Pathway*[S]

Received for publication, July 7, 2010, and in revised form, December 16, 2010 Published, JBC Papers in Press, December 20, 2010, DOI 10.1074/jbc.M110.161489

Estefanía Moreno[‡], Hanne Hoffmann[§¶], Marta Gonzalez-Sepúlveda[§], Gemma Navarro[‡], Vicent Casadó[‡], Antoni Cortés[‡], Josefa Mallol[‡], Michel Vignes[¶], Peter J. McCormick[‡1], Enric I. Canela[‡], Carme Lluís[‡], Rosario Moratalla[‖], Sergi Ferré[**], Jordi Ortiz[§2], and Rafael Franco[‡ ‡‡2,3]

From the [‡]Centro de Investigación Biomédica en Red sobre Enfermedades Neurodegenerativas, and Department of Biochemistry and Molecular Biology, Faculty of Biology, University of Barcelona, Diagonal 645, 08028 Barcelona, Spain, the [§]Neuroscience Institute and Department of Biochemistry and Molecular Biology, Faculty of Medicine, Universitat Autónoma de Barcelona, 08193 Bellaterra, Spain, [¶]UMR 5247 The Max Mousseron Biomolecules Institute, CNRS, University of Montpellier 1 and 2, University of Montpellier 2, 34095 Montpellier, France, [‖]Instituto Cajal, Consejo Superior de Investigaciones Científicas, Madrid, Spain, the [**]National Institute on Drug Abuse, Intramural Research Program, National Institutes of Health, Department of Health and Human Services, Baltimore, Maryland 21224, and the [‡‡]Centro de Investigación Médica Aplicada, Universidad de Navarra, Pio XII 55, 31008 Pamplona, Spain

Previously, using artificial cell systems, we identified receptor heteromers between the dopamine D_1 or D_2 receptors and the histamine H_3 receptor. In addition, we demonstrated two biochemical characteristics of the dopamine D_1 receptor-histamine H_3 receptor heteromer. We have now extended this work to show the dopamine D_1 receptor-histamine H_3 receptor heteromer exists in the brain and serves to provide a novel link between the MAPK pathway and the GABAergic neurons in the direct striatal efferent pathway. Using the biochemical characteristics identified previously, we found that the ability of H_3 receptor activation to stimulate p44 and p42 extracellular signal-regulated MAPK (ERK 1/2) phosphorylation was only observed in striatal slices of mice expressing D_1 receptors but not in D_1 receptor-deficient mice. On the other hand, the ability of both D_1 and H_3 receptor antagonists to block MAPK activation induced by either D_1 or H_3 receptor agonists was also found in striatal slices. Taken together, these data indicate the occurrence of D_1-H_3 receptor complexes in the striatum and, more importantly, that H_3 receptor agonist-induced ERK 1/2 phosphorylation in striatal slices is mediated by D_1-H_3 receptor heteromers. Moreover, H_3 receptor-mediated phospho-ERK 1/2 labeling co-distributed with D_1 receptor-containing but not with D_2 receptor-containing striatal neurons. These results indicate that D_1-H_3 receptor heteromers work as processors integrating dopamine- and histamine-related signals involved in controlling the function of striatal neurons of the direct striatal pathway.

The striatum is the main input structure of the basal ganglia, which are subcortical structures involved in the processing of information related to the performance and learning of complex motor acts. It is widely accepted that dopamine receptor subtypes, which are fundamental for motor control and are implicated in numerous neuropsychiatric disorders, are largely segregated in the two subtypes of medium spiny neurons (MSNs),[4] the most populated neuronal type in the striatum. Dopamine D_2 receptors (D_2Rs) are mostly localized in the striatopallidal MSNs, which express the peptide enkephalin and which gives rise to the indirect striatal efferent pathway, whereas dopamine D_1 receptors (D_1Rs) are mostly expressed by the striatonigral MSNs, which express substance P and dynorphin and constitute the direct striatal efferent pathway (1, 2). Dopaminergic drugs activate the ERK transduction pathway, which is involved in basic physiological processes and in synaptic plasticity (3). In the dopamine-depleted striatum, ERK signaling is implicated in the development of L-DOPA-induced dyskinesia. Thus, in dopamine-denervated mice, L-DOPA activates ERK signaling specifically in D_1Rs containing striatonigral MSNs but not in D_2Rs containing striatopallidal MSNs (4). This regulation may result in ERK-dependent changes in striatal plasticity leading to dyskinesia.

Histamine is an important regulatory transmitter in the nervous system involved in the sleep/wake cycle, attention, memory, and other functions. Four histamine receptor types (H_1R–H_4R) have been cloned. H_3Rs are expressed in abundance in the brain and high densities are particularly found in the striatum (5–7). H_3Rs were first identified as autoreceptors (8), but they were later found to act as heteroreceptors (9).

* This study was supported by Grants SAF2008-00146, SAF2008-03229-E, SAF2009-07276, SAF2006-08240, and SAF2009-12510 from the Spanish Ministerio de Ciencia y Tecnología, the Centre National de la Recherche Scintifique, the French Ministry of Research and Higher Education, Red de Transtornos Adictivos RD06/0001/0015, Grant 060110 from Fundació La Marató de TV3 and the Intramural Funds of the National Institute on Drug Abuse.

[S] The on-line version of this article (available at http://www.jbc.org) contains supplemental Fig. 1.

[1] A Ramon y Cajal investigator.

[2] Both authors contributed equally to this article.

[3] To whom correspondence should be addressed: Centro de Investigación Médica Aplicada, University of Navarra, Pio XII, 55, 31008 Pamplona, Italy. Tel.: 34-948194700; Fax: 34-948194715; E-mail: rfranco@unav.es.

[4] The abbreviations used are: MSN, medium spiny neurons; D_2R, dopamine D_2 receptor; H_1R, histamine H_1 receptor; D_1R, dopamine D_1 receptor; RAMH, R(−)-α-methylhistamine dihydrochloride.

The major localization of striatal H_3Rs is postsynaptic (5, 10), and most probably in both subtypes of MSNs (6, 10). Histamine, by means of interactions with striatal H_3Rs, plays an important role in the modulation of dopamine neurotransmission (11–14). At the behavioral level, it was shown that stimulation of postsynaptic H_3R counteracts the motor activation induced by D_1R and D_2R agonists in reserpinized mice (14). These interactions may be related to the ability of H_3Rs to form heteromers with dopamine receptors. In fact, D_1R-H_3R and D_2R-H_3R heteromerization was demonstrated by biophysical techniques in mammalian cells (14, 15). However, their presence in the brain remained to be demonstrated. In addition, if H_3Rs form heteromers with both D_1R and D_2R, is there a functional difference between these two receptor heteromer pairs? One might expect that because the D_1R and D_2R receptors are found in two different neuronal pathways that the different heteromers might confer different properties. Here, we have explored this idea by taking advantage of unique properties of the D_1R-H_3R heteromers to provide evidence for their presence in rodent brain. Previously, using an *in vitro* cell system, we found an important feature of the D_1R-H_3R heteromer is that H_3R agonists only activate ERK 1/2 in a receptor heteromer context, but not in cells expressing H_3Rs without D_1R (15). Here, by taking advantage of this distinct ERK 1/2 signaling characteristic, we demonstrate the occurrence of D_1R-H_3R heteromers in rodent striatum. Despite H_3Rs being expressed in both D_1R and D_2R containing neurons, histamine-receptor-mediated phosphorylation of the ERK 1/2 kinase occurred only in neurons expressing D_1R and not in those with D_2R. Thus, D_1-H_3 receptor heteromers confer a direct link to MAPK activation within the GABAergic neurons of the direct striatal efferent pathway.

EXPERIMENTAL PROCEDURES

Animals—Sprague-Dawley male rats, 7–9 weeks old and weighing 200–250 g, were provided by the Animal Service of the Universidad Autónoma de Barcelona (Barcelona, Spain). Six-to-eight-month-old wild-type littermates and dopamine D_1 receptor knock-out C57BL6 male mice, weighing 25–30 g, were provided by Instituto Cajal (Consejo Superior de Investigaciones Científicas; Madrid, Spain) and generated by homologous recombination as described previously (16). Rats (2 per cage) or mice (five per cage) were housed in a temperature (21 ± 1 °C) and humidity-controlled (55 ± 10%) room with a 12:12 h light/dark cycle (light between 08:00 and 20:00 h) with food and water *ad libitum*. Animal procedures were conducted according to standard ethical guidelines (European Communities Council Directive 86/609/EEC) and approved by the local (Universidad Autónoma de Barcelona or Consejo Superior de Investigaciones Científicas) ethical committee.

Cell Culture and Membrane Preparation—SK-N-MC/H_3 cells were grown in Eagle's minimal essential medium, supplemented with 10% FBS, 50 units/ml penicillin, 50 μg/ml streptomycin, nonessential amino acids, 2 mmol/liter L-glutamine, and 50 μg/ml sodium pyruvate at 37 °C in a humidified atmosphere of 5% CO_2 to 80% confluence. The SK-N-MC cells stably expressing the human H_3R (SK-N-MC/H_3) were provided by Johnson & Johnson Pharmaceutical Research & Development, L.L.C. Cells were disrupted with a Polytron homogenizer (PTA 20 TS rotor, setting 3; Kinematica, Basel, Switzerland) in 50 mM Tris-HCl buffer, pH 7.4, containing a protease inhibitor mixture (1/1000; Sigma). The cellular debris was removed by centrifugation at 13,000 × *g* for 5 min at 4 °C, and membranes were obtained by centrifugation at 105,000 × *g* for 1 h at 4 °C. Membranes were lysed in 50 mM Tris-HCl, pH 7.4, containing 50 mM NaF, 150 mM NaCl, 45 mM β-glycerophosphate, 1% Triton X-100, 20 μM phenylarsine oxide, 0.4 mM $NaVO_4$, and protease inhibitor mixture to be processed by Western blot.

Brain Slice Preparation—Rats and mice were decapitated with a guillotine, and the brains were rapidly removed and placed in ice-cold oxygenated (O_2/CO_2: 95/5%) Krebs-HCO_3^- buffer (124 mM NaCl, 4 mM KCl, 1.25 mM NaH_2PO_4, 1.5 mM $MgCl_2$, 1.5 mM $CaCl_2$, 10 mM glucose, and 26 mM $NaHCO_3$, pH 7.4). The brains were sliced at 4 °C in a brain matrix (Zivic Instruments, Pittsburgh, PA) into 0.5-mm coronal slices. Slices were kept at 4 °C in Krebs-HCO_3^- buffer during the dissection of the striatum. Each slice was transferred into an incubation tube containing 1 ml of ice-cold Krebs-HCO_3^- buffer. The temperature was raised to 23 °C and after 30 min, the medium was replaced by 2 ml Krebs-HCO_3^- buffer (23 °C). The slices were incubated under constant oxygenation (O_2/CO_2: 95/5%) at 30 °C for 4–5 h in an Eppendorf Thermomixer (5 Prime, Inc., Boulder, CO). The media was replaced by 200 μl of fresh Krebs-HCO_3^- buffer and incubated for 30 min before the addition of ligands.

ERK Phosphorylation Assays—Striatal slices were incubated in the presence of the indicated concentrations of histamine H_3 or dopamine D_1 receptor ligands, prepared in Krebs-HCO_3^- buffer. After the indicated incubation period, the solution was discarded, and slices were frozen on dry ice and stored at −80 °C. Slices were lysed by the addition of 500 μl of ice-cold lysis buffer (50 mM Tris-HCl pH 7.4, 50 mM NaF, 150 mM NaCl, 45 mM β-glycerophosphate, 1% Triton X-100, 20 μM phenylarsine oxide, 0.4 mM $NaVO_4$, and protease inhibitor mixture). Cellular debris was removed by centrifugation at 13,000 × *g* for 5 min at 4 °C, and protein was quantified by the bicinchoninic acid method using bovine serum albumin dilutions as standard. To determine the level of ERK1/2 phosphorylation, equivalent amounts of protein (10 μg) were separated by electrophoresis on a denaturing 10% SDS-polyacrylamide gel and transferred onto PVDF-FL membranes. Odyssey blocking buffer (LI-COR Biosciences, Lincoln, Nebraska) was then added, and membranes were rocked for 90 min. Membranes were then probed with a mixture of a mouse antiphospho-ERK 1/2 antibody (1:2500, Sigma) and rabbit anti-ERK 1/2 antibody (1:40,000, Sigma) for 2–3 h. The 42 and 44 kDa bands corresponding to ERK 1 and ERK 2 were visualized by the addition of a mixture of IRDye 800 (anti-mouse) antibody (1:10,000, Sigma) and IRDye 680 (anti-rabbit) antibody (1:10,000, Sigma) for 1 h and scanned by the Odyssey infrared scanner (LI-COR Biosciences). Bands densities were quantified using the scanner software and exported to Microsoft Excel. The level of phosphorylated ERK 1 and phosphorylated ERK 2 was normalized for differences in loading using the total ERK 1/2 protein band intensities.

Immunohistochemistry—Striatal slices were incubated with the indicated H_3R ligands in Krebs-HCO_3^- buffer for 10 min and fixed with 4% paraformaldehyde solution (Antigenfix, DiaPath) for 1 h at room temperature with gentle agitation. The slices were then washed in TBS (50 mM Tris-HCl, 0.9% NaCl, pH 7.8), treated 5 min with 1% Na_2BH_4 dissolved in TBS, followed by successive TBS washes until all Na_2BH_4 was eliminated. Finally, the slices were cryopreserved in a 30% sucrose solution overnight at 4 °C and stored at −20 °C until sectioning. 15-μm-thick coronal sections were cut on a freezing cryostat (Leica Jung CM-3000) and mounted on slide glass (three control and three treated coronal sections in each slide; STAR FROST PLUS, DELTALAB). Coronal sections were thawed at 4 °C, washed in TBS, and rocked in 7% normal donkey serum (SND, Sigma) in TBS for 1 h at 37 °C in a humidified atmosphere. Coronal sections were then incubated overnight at 4 °C in a humidified atmosphere with the primary antibodies: rabbit antiphospho-Thr^{202}/Tyr^{204} ERK 1/2 antibody (1:300, Cell Signaling Technology, Danvers, MA), guinea pig anti-D_1 antibody (1:100, Frontier Institute, Ishikari, Hokkaido, Japan) or guinea pig anti-D_2 antibody (1:100, Frontier Institute, Ishikari, Hokkaido, Japan) alone or in combination in a solution with 0.1% TBS-Tween, 0.1% BSA-acetylated (Aurion), 7% SND (250 μl per slide). The specificity of these dopamine receptor antibodies has been previously shown by preabsorption tests with the antigen peptides and by mutually exclusive pattern and triple labeling in immunohistochemistry (17) and by Western blot (see "Results"). Coronal sections were washed in 0.05% TBS-T and left for 2 h at room temperature in a humidified atmosphere with the corresponding secondary antibodies: chicken anti-rabbit (1:200, Alexa Fluor 594, Invitrogen) and goat anti-guinea pig (1:200, Alexa Fluor 488, Invitrogen) in a solution with TBS-Tween 0.1%, BSA acetylated 0.1%, SND 7%, and then washed in TBS-T 0.05%, followed by a single wash in TBS before mounting in Mowiol medium (Calbiochem), covered with a glass, and left to dry at 4 °C for 24 h. Single and double immunostained slices were observed and imaged in a Leica SP2 confocal microscope (Leica Microsystems, Mannheim, Germany). Images were opened and processed with ImageJ confocal microscopy program and a Adobe Photoshop program (version 5.5; Seattle, WA). Double-labeled cells (cells stained for phospho-ERK 1/2 and D_1 or D_2 receptors) were counted in a total of two to three nonoverlapping fields of 45 coronal sections from 4 to 5 slices treated with medium (control), 1 μM RAMH, or 1 μM imetit.

Coronal sections from nontreated slices (six control coronal sections in each slide) were used for double-immunohistochemistry using rabbit anti-H_3R antibody (1:200, Chemicon, Billerica, MA) and guinea pig anti-D_1R antibody or guinea pig anti-D_2R antibody as primary antibodies and goat anti-rabbit-peroxidase (1:200, Thermo Scientific, Fremont, CA) and goat anti-guinea pig (1:200, Alexa Fluor 488, Invitrogen) as secondary antibodies by the same procedure as described above. In this case, the amplification system for the red fluorophore, TSA-cyanine 3 (1:100, Tyramide Signal Amplification, PerkinElmer Life Science) was used as described in the TSA Plus fluorescence amplification kit, before mounting in Mowiol medium. Double-labeled cells (cells stained for H_3 and D_1 or D_2 receptors) were counted in a total of two to three nonoverlapping fields of 15 coronal sections from four to five slices. In all cases, we did not observe staining in the absence of the primary antibodies.

Coimmunoprecipitation—The rat striatal tissue was disrupted with a Polytron homogenizer in 50 mM Tris-HCl buffer, pH 7.4, containing a protease inhibitor mixture (1/1000, Sigma). The cellular debris was removed by centrifugation at 13,000 × *g* for 5 min at 4 °C, and membranes were obtained by centrifugation at 105,000 × *g* for 1 h at 4 °C. Membranes were washed two more times at the same conditions and were solubilized by homogenization in ice-cold immunoprecipitation buffer (phosphate-buffered saline, pH 7.4, containing 1% (v/v) Nonidet P-40) and incubated for 30 min on ice before centrifugation at 105,000 × *g* for 1 h at 4 °C. The supernatant (1 mg/ml of protein) was processed for immunoprecipitation as described in immunoprecipitation protocol using a Dynabeads® Protein G kit (Invitrogen). Protein was quantified by the bicinchoninic acid method (Pierce) using bovine serum albumin dilutions as standard. Immunoprecipitates were carried out with rat anti-D_1 receptor antibody (1:1000, Sigma) or rabbit anti-D_2 receptor antibody (1:1000, Millipore, Billerica, MA) As negative control anti-calnexin antibody was used (1:1000, BD Biosciences Pharmingen). Immunoprecipitates were separated on a denaturing 10% SDS-polyacrylamide gel and transferred onto PVDF membranes. Membranes were proved with the primary antibodies guinea pig anti-D_1 antibody (1:1000, Frontier Institute, Ishikari, Hokkaido, Japan), guinea pig anti-D_2 antibody (1:1000, Frontier Institute) or goat anti-H_3R antibody (1:500, Santa Cruz Biotechnology, Santa Cruz, CA) and the secondary antibodies goat anti-guinea pig-peroxidase (1:20,000, Sigma) and donkey anti-goat-peroxidase (1:20,000, Jackson ImmunoResearch Laboratories, West Grove, PA). Bands were visualized with a LAS-3000 (Fujifilm). Analysis of detected bands was performed by Image Gauge software (version 4.0) and Multi Gauge software (version 3.0).

RESULTS

D_1R and H_3R Are Functionally Coupled to MAPK Signaling Pathway in Brain Striatal Slices—To establish whether D_1R and H_3R are functionally coupled to the MAPK pathway in rat striatum, slices were treated with a D_1R or an H_3R agonist, and ERK 1/2 phosphorylation was assayed as described under "Experimental Procedures." The time response curve obtained after treatment with 10 μM SKF 38393 (D_1R agonist) or 0.1 μM imetit (H_3R agonist) showed that phosphorylation peaked at 10 min (Fig. 1*a*). Therefore, all subsequent assays were analyzed at 10 min of drug treatment. Dose-response curves for different D_1R or H_3R agonists are displayed in Fig. 1*b*. Both SKF 81297 and SKF 38393 (full and partial D_1R agonists, respectively) were able to increase ERK 1/2 phosphorylation; SKF 81297 was more potent than SKF 39393. RAMH and imetit (H_3R agonists) also increased ERK 1/2 phosphorylation, with imetit being more potent than RAMH. The results show that striatal slices contain D_1R and H_3R functionally coupled to MAPK signaling.

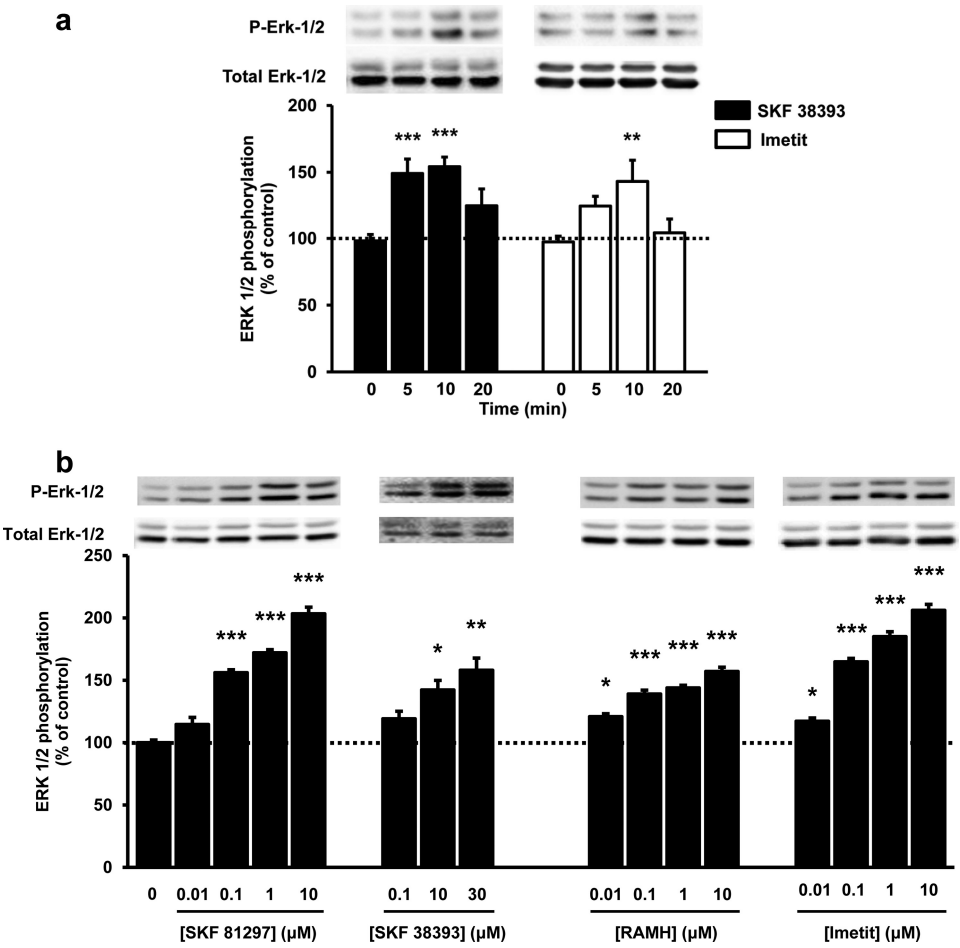

FIGURE 1. **H_3R and D_1R agonists induced ERK 1/2 phosphorylation in rat striatal slices.** *a*, slices were treated with 10 μM SKF 38393 (*black*) or 1 μM imetit (*white*). *b*, slices were treated for 10 min with different SKF 81297, SKF 38393, RAMH, or imetit concentrations. ERK 1/2 phosphorylation was determined as described under "Experimental Procedures." The immunoreactive bands from five to 27 (*a*) or 19 to 24 (*b*) slices obtained from three to 14 (*a*) or six to nine (*b*) animals were quantified, and values represent the mean ± S.E. of the percentage of phosphorylation relative to basal levels of untreated slices (100%). Significant differences were calculated by one-way analysis of variance with post hoc Bonferroni's multiple tests and *, **, and *** correspond to $p < 0.05$, $p < 0.01$, and $p < 0.001$, respectively, as compared with nontreated samples (control). A representative Western blot is shown in each panel (*top*).

H_3R Agonist-induced ERK 1/2 Phosphorylation in Striatal Slices Is Mediated by D_1R-H_3R Heteromers—A cross-antagonism between D_1Rs and H_3Rs has been demonstrated previously in heterologous cell systems. This cross-antagonism only occurs in D_1R-H_3R-heteromer-containing cells and consists of both the ability of D_1R antagonists to block the effect of H_3R agonists and, conversely, the ability of H_3R antagonists to block the effect of D_1R agonists (15). To test whether this phenomenon also occurs *in vivo*, rat striatal slices were incubated with D_1R or H_3R agonists (SKF 81297 or RAMH, respectively) in the presence of either D_1R or H_3R antagonists (SCH 23390 or thioperamide, respectively). The results reproduced the cross-antagonism found in the heterologous cell system (Fig. 2). ERK 1/2 phosphorylation induced by RAMH (0.1 μM) was not only blocked by thioperamide (10 μM) but also by SCH 23390 (10 μM) (Fig. 2*a*). Similarly, ERK 1/2 phosphorylation induced by SKF 81297 (0.1 μM) was blocked by both SCH23390 and thioperamide (10 μM in both cases) (Fig. 2*b*). As a control, activation of striatal serotonin receptors (with 0.2 μM of serotonin) significantly induced ERK 1/2 phosphorylation, but the effect was not modified by either SCH23390 or thioperamide (10 μM in both cases) (Fig. 2, *c* and *d*). These results provide evidence for the expression D_1R-H_3R heteromers in the striatum. Another characteristic of the D_1R-H_3R heteromer is that it allows H_3R agonists to activate MAPK signaling (15). We decided to investigate whether this heteromer characteristic persisted *in vivo* using transgenic mice lacking D_1Rs. When H_3R-mediated MAPK signaling was investigated in striatal slices from transgenic mice lacking the D_1Rs and in wild-type littermate controls displaying the same genetic background, RAMH (0.1 μM) was unable to induce ERK 1/2 phosphorylation, whereas a strong signal was obtained in slices from wild-type littermate controls displaying the same genetic background (Fig. 3). In addition in wild-type animals, RAMH-induced ERK 1/2 phosphorylation was blocked by both thioperamide (10 μM) and SCH 23390 (10 μM) (Fig. 3). These results indicate that H_3R agonist-induced ERK 1/2 phosphorylation in striatal slices is mediated by D_1R-H_3R heteromers.

To provide further insight on the function of striatal D_1R and H_3R receptors coexpressed in striatal neurons, ERK 1/2

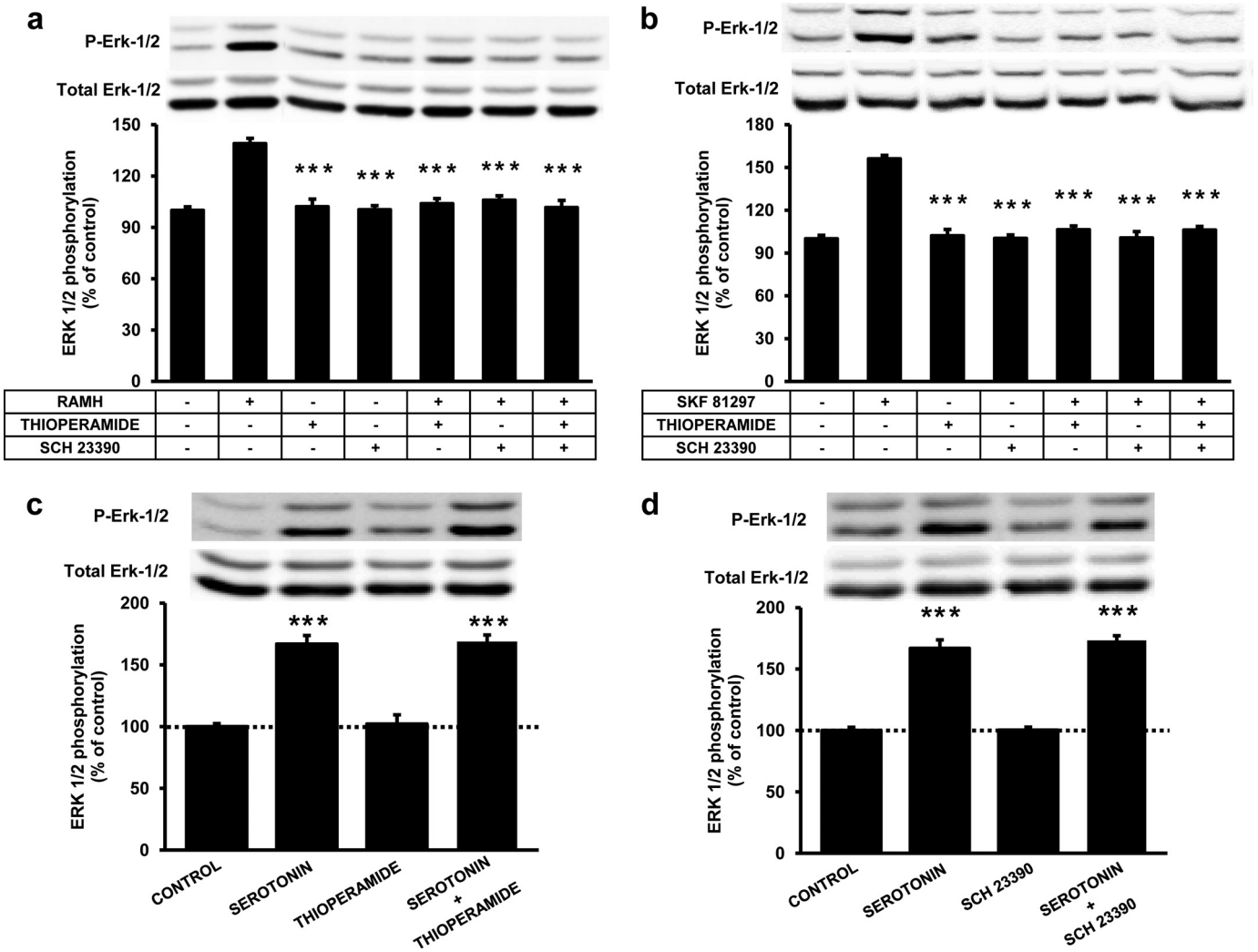

FIGURE 2. **Effect of H_3R and D_1R antagonists on agonist-induced ERK 1/2 phosphorylation in rat striatal slices.** Slices were preincubated with medium or with 10 μM thioperamide, 10 μM SCH 23390, or both for 20 min prior to the addition of 0.1 μM RAMH (*a*) or 0.1 μM SKF 81297 (*b*) followed by a further incubation of 10 min. In *c* and *d*, slices were preincubated for 20 min with medium or with 10 μM thioperamide (*c*) or 10 μM SCH 23390 (*d*) prior to the addition of 0.2 μM serotonin followed by a further incubation of 10 min. ERK1/2 phosphorylation was determined as described under "Experimental Procedures." The immunoreactive bands from 12 to 21 (*a* and *b*) or 10 to 14 (*c* and *d*) slices obtained from 8 to 10 (*a* and *b*) or 4 to 6 (*c* and *d*) animals were quantified, and values represent the mean ± S.E. of the percentage of phosphorylation relative to basal levels found in untreated slices (100%). Significant differences were calculated by one-way analysis of variance with post hoc Bonferroni's multiple tests (***, $p < 0.001$, as compared with the first treatment in *a* and *b*, or to the basal in *c* and *d*). A representative Western blot is shown in each panel (*top*).

activation was studied in rat striatal slices in the presence of agonists for the two receptors. This would mimic the situation when the two neurotransmitters histamine and dopamine are simultaneously impacting a given GABAergic neuron. Interestingly, the effect of the D_1R agonist SKF 81297 (10 μM) was significantly counteracted by the H_3R agonist, RAMH (1 μM). Furthermore, the combination of RAMH (10 μM) and SKF 81297 (1 μM) produced a significantly weaker effect than that of either drug alone (Fig. 4), indicating the existence in striatal neural circuits of an agonist-induced D_1R-H_3R reciprocal negative cross-talk.

Selective D_1R-H_3R Heteromer-mediated Effects only in Striatal Neurons of Direct Pathway—Dopamine receptors are segregated in the two main types of GABAergic striatal efferent neurons: dynorphinergic neurons of the direct pathway expressing D_1Rs and enkephalinergic neurons of the indirect pathway expressing dopamine D_2Rs. Evidence supporting the presence of H_3R in both types of neurons had been obtained previously by autoradiography and lesion studies (5) and by *in situ* hybridization (10). Accordingly, by double immunohistochemistry using H_3R and either D_1R or D_2R antibodies, we found H_3R immunostaining in cells labeled with either D_1R or D_2R antibodies (Fig. 5). In fact, 95 ± 12% of D_1R stained neurons or 89 ± 15% of D_2R stained neurons showed H_3R staining (Fig. 6*a*). Thus, co-expression of D_1R and H_3R in GABAergic neurons of the direct pathway and co-expression of D_2R and H_3R in GABAergic neurons of the indirect pathway was found. We have described previously that both D_1R and D_2R may form heteromers with H_3R in living cells (14, 15). To test D_1R-H_3R and D_2R-H_3R heteromer expression in the rat striatum, co-immunoprecipitation experiments were carried out. The immunoprecipitates with the anti-D_1R antibody (Fig. 7*a*) or with the anti-D_2R antibody (Fig. 7*b*) were not stained in a Western blot using anti-D_2R or anti-D_1R anti-

bodies respectively, showing the specificity of the antibodies. Interestingly, specific H_3R staining was detected by Western blot in both immunoprecipitates using anti-D_1R or anti-D_2R antibodies but not with an irrelevant antibody (Fig. 7*c*). These results corroborate the expression of D_1R-H_3R heteromers in the neurons of the direct pathway and suggest the expression of D_2R-H_3R heteromers in the neurons of the indirect pathway.

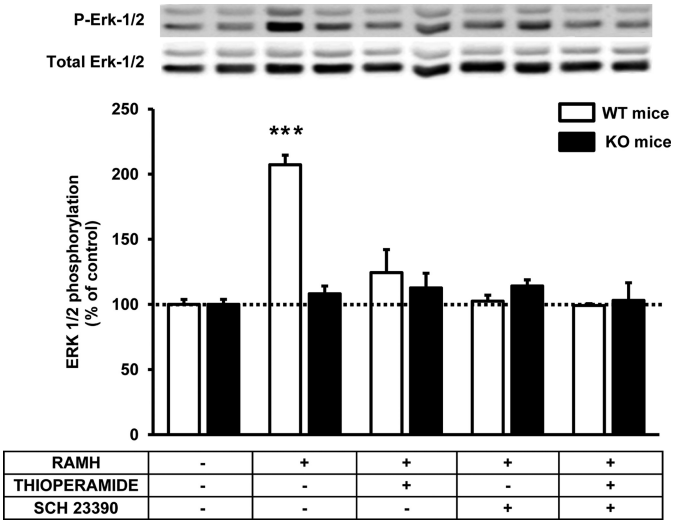

FIGURE 3. **H_3R agonist-induced ERK 1/2 phosphorylation in striatal slices from wild-type and dopamine D_1R knock-out mice.** Wild-type (*white*) or D_1R knock-out mice (*black*) slices were treated for 10 min with 0.1 μM RAMH or for 10 min with 10 μM thioperamide and/or 10 μM SCH 23390 prior to the addition of 0.1 μM RAMH and incubation for further 10 min. ERK 1/2 phosphorylation was determined as described under "Experimental Procedures." For each treatment, the immunoreactive bands from four to six slices from a total six wild-type and nine knock-out animals were quantified, and values represent the mean ± S.E. of the percentage of phosphorylation relative to basal levels found in untreated slices (100%). No significant differences were obtained between the basal levels of the wild-type and the D_1R knock-out mice, and no significant differences were observed between basal and slices treated (20 min) with 10 μM thioperamide or 10 μM SCH 23390. Significant treatment and genotype effects were analyzed by a bifactorial analysis of variance followed by post hoc Bonferroni's tests. There were significant genotype, treatment, and interaction effects, explained by the ability of RAMH to strongly and selectively induce ERK 1/2 phosphorylation in wild-type mice (***, $p < 0.001$, as compared with knock-out mice). A representative Western blot is also displayed (*top*).

In striatal slices incubated with 1 μM imetit and subjected to immunohistochemistry, we observed that imetit-induced ERK 1/2 phosphorylation occurs in a high number of neurons stained using the anti-D_1R antibody, but only in a small number of neurons stained using the anti-dopamine D_2R antibody (Fig. 8). In fact, 85 ± 7% of phospho-ERK 1/2-positive neurons displayed specific D_1 receptor immunostaining, whereas only 23 ± 5% of phospho-ERK 1/2-positive neurons were positive for D_2 receptor labeling (Fig. 6*b*). It should be noted that despite D_2R-H_3R heteromers may play a role in this signaling pathway, neurons containing both the D_1R and D_2R may exist in the striatum (18). Similar results were obtained in striatal slices incubated with 1 μM RAMH (results not shown). Furthermore, the effect of H_3R agonists in striatal slices was independent of changes in presynaptic neurotransmitter release (*e.g.* dopamine or histamine), which could potentially contribute to trigger ERK 1/2 phosphorylation in D_1R-expressing cells. In fact, the presence of 1 μM tetrodotoxin affected neither the D_1R agonist nor the H_3R agonist-induced ERK 1/2 phosphorylation (supplemental Fig. 1). Collectively, these results demonstrate that histamine-induced MAPK pathway activation in striatal slices is specifically mediated by the D_1R and H_3R heteromers present in neurons of the direct pathway, but not by the H_3Rs localized in the indirect pathway or as autoreceptors or heteroceptors in neighboring nerve terminals.

DISCUSSION

We have previously described that not only D_1R but also D_2R may form heteromers with H_3R in living cells (14, 15). Here, it is demonstrated that both D_1R and D_2R co-immunoprecipitate H_3R from rat striatum supporting the expression

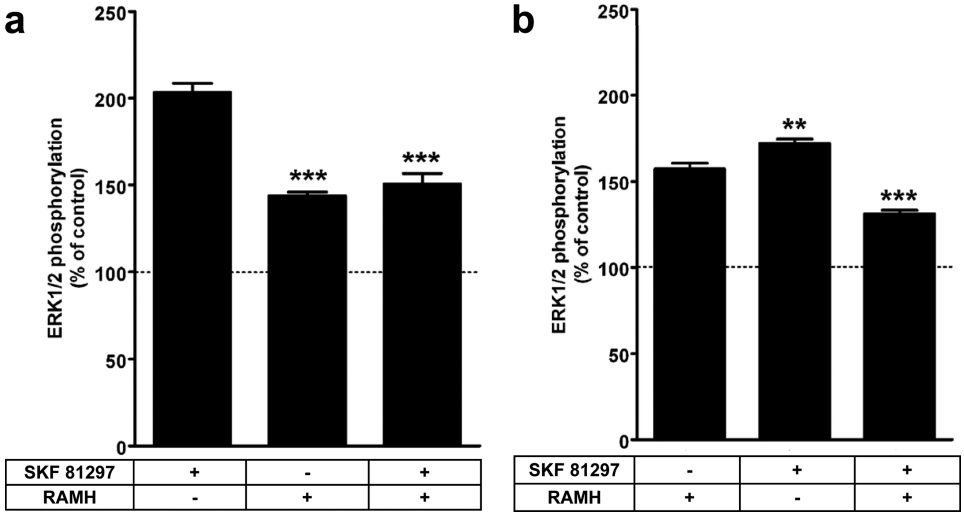

FIGURE 4. **Negative cross-talk between D_1Rs and H_3R receptors on ERK 1/2 phosphorylation in rat striatal slices.** Slices were treated for 10 min with 10 μM SKF 81297 and/or 1 μM RAMH (*a*) or 10 μM RAMH and/or 1 μM SKF 81297 (*b*). ERK 1/2 phosphorylation was determined as described under "Experimental Procedures." The immunoreactive bands from 10 to 24 (*a*) or eight to 23 (*b*) slices obtained from four to six animals were quantified, and values represent the mean ± S.E. of the percentage of phosphorylation relative to basal levels found in untreated slices (100%). Significant differences were calculated by one-way analysis of variance with post hoc Bonferroni's multiple tests. (** and ***, $p < 0.01$ and $p < 0.001$, respectively, as compared with 10 μM SKF 81297 in (*a*) or 10 μM RAMH in (*b*)).

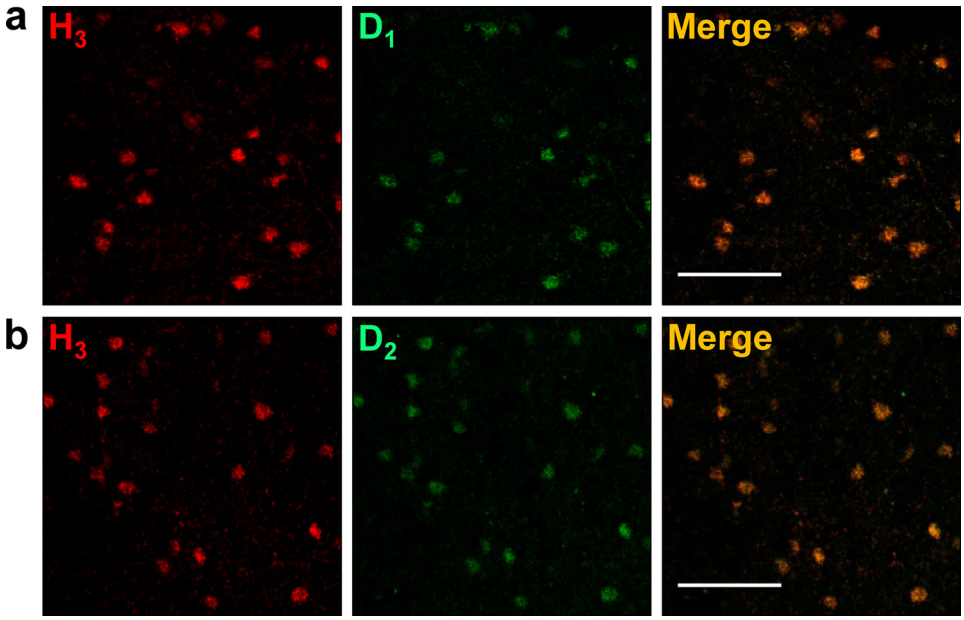

FIGURE 5. **Co-localization between H_3R and D_1R or D_2R in striatal MSNs.** Confocal microscope representative images of coronal sections from striatal slices are shown. Slices were labeled with anti-H_3R antibody (*red*). Labeling (*green*) using an anti-D_1R antibody (*a*) or an anti-D_2R antibody (*b*) is also shown. In *a* and *b*, colocalization is shown in *yellow*. *Scale bars*, 60 μm.

of D_1R-H_3R and D_2R-H_3R heteromers in the neurons of the direct and indirect striatal efferent pathways, respectively. From our earlier work, it was unclear whether D_1R-H_3R and D_2R-H_3R heteromers were engaging similar signaling pathways in the two different neuronal populations or whether there was a functional difference that might help delineate the direct and indirect pathways of the striatum via the existence of these heteromers. The data presented in this paper indicate that D_1R-H_3R heteromers in the striatonigral GABAergic neurons of the direct pathway, but not the H_3R receptors in the indirect pathway, allow direct histaminergic activation of the MAPK pathway.

Biophysical techniques can provide strong support for the existence of receptor heteromers in artificial cell systems (19, 20), but, as these techniques are difficult to perform in intact tissues, obtaining evidence for naturally occurring heteromer expression remains a significant challenge. For many receptor heteromers, we depend on an indirect approach for their identification in native tissues, which relies on the discovery of a characteristic signature of the heteromer. This characteristic, which is usually identified in a heterologous cell system, may be then used as a "fingerprint" to demonstrate the presence of the heteromer in the native tissue (21–24). A specific characteristic of the D_1R-H_3R heteromer, previously identified in transfected cells is cross-antagonism (15), *i.e.* the ability of both D_1R and H_3R antagonists to block the effect of either D_1R or H_3R agonists. This phenomenon, in which an antagonist of one of the receptor units in the receptor heteromer blocks signaling originated by ligand binding to the other receptor unit in the heteromer, has also been observed with other receptor heteromers, such as the cannabinoid CB_1-orexin OX_1 receptor heteromer (25). Significantly, the same D_1R-H_3R cross-antagonism on MAPK signaling, which was described in transfected cells (15), was observed in rat striatal slices (Fig. 2), strongly supporting the occurrence of D_1R-H_3R heteromers in the rodent striatum. Of note, a further characteristic of the D_1R-H_3R heteromer is its ability to allow the activation of the MAPK cascade by H_3R-selective agonists, which otherwise cannot drive this signaling pathway (15). In fact, H_3R agonist-induced ERK 1/2 phosphorylation was demonstrated in striatal slices of wild-type but not of D_1R knockout mice, indicating the occurrence of D_1R-H_3R heteromers in the rodent striatum. As the H_3R agonist was unable to activate MAPK signaling in slices from D_1R-deficient mice (Fig. 3) it is likely that only neurons containing both H_3R and D_1R are able to link histaminergic neurotransmission to the MAPK cascade. Interestingly, although H_3R were found to be co-expressed with D_1R- and D_2R-containing neurons, the H_3R-mediated phospho-ERK labeling only co-distributed with D_1R- but not with D_2R-containing neurons (Figs. 5 and 8) and was not dependent on neurotransmitter release from neighboring cells.

The results obtained with co-administration of D_1R and H_3R agonists suggest that the D_1R-H_3R heteromer works as a processor that integrates dopamine and histamine-related signals, and its output consists of quantitatively different activation of the MAPK pathway. Strong MAPK signaling was obtained with either D_1R or H_3R activation, but a significantly weaker MAPK signaling was obtained upon co-activation of both receptors. Thus, at very low dopamine concentrations, histamine can foster MAPK signaling by activating H_3Rs in D_1R-H_3R-coexpressing neurons. In contrast, when the two neurotransmitters are present, the MAPK activation in the striatonigral MSN would be repressed. Because the MAPK pathway is considered critical to activity-dependent changes underlying synaptic strengthening (26), our results predict that not only dopamine but also histamine plays an important role in MAPK-dependent neuroplasticity in the striatonigral MSN.

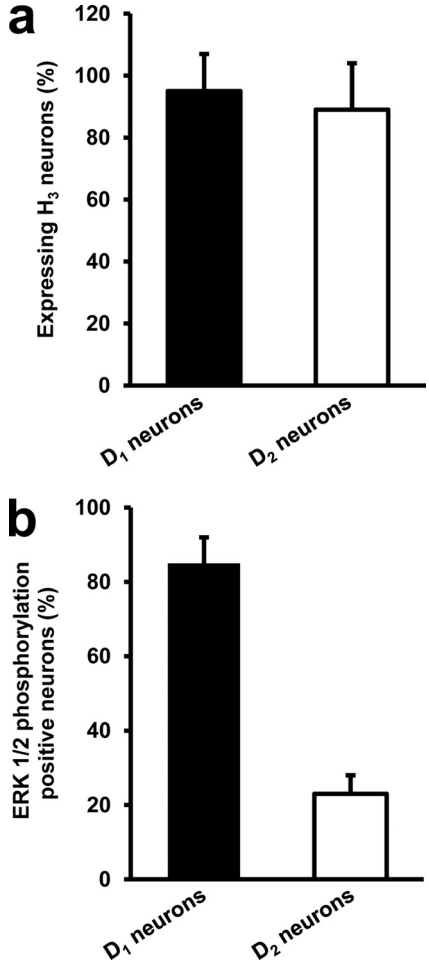

FIGURE 6. **Quantification of colocalization in confocal microscope images.** Quantification of H_3R expression (*a*) or 1 μM imetit-induced ERK 1/2 phosphorylation (*b*) in neurons expressing D_1R (D_1 neurons) or D_2R (D_2 neurons). Values are mean ± S.E. of the percentage of double-labeled cells (cells stained for $H_3R$and D_1Ror D_2R in *a* or cells stained for imetit-induced phospho-ERK 1/2 and D_1Ror D_2R in *b*) were counted in a total of two to three nonoverlapping fields of 15 (*a*) or 45 (*b*) coronal sections from four to five slices.

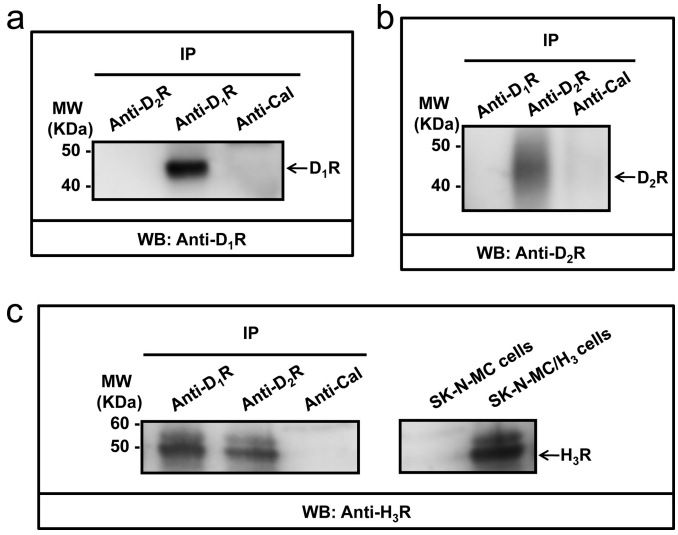

FIGURE 7. **Co-immunoprecipitation of H_3R and D_1R or D_2R.** Rat striatal membranes were solubilized and processed for immunoprecipitation as described under "Experimental Procedures" using rat anti-D_1R antibody, rabbit anti-D_2R antibody, or rabbit anti-calnexin antibody as negative control. As positive controls and to test the specificity of dopamine receptors antibodies, immunoprecipitates were analyzed by SDS-PAGE and immunoblotted using guinea pig anti-D_1R antibody (*a*) or guinea pig anti-D_2R antibody (*b*). To test the co-immunoprecipitation, immunoprecipitates were blotted with goat anti-H_3R antibody (*c*). The *right panel* in *c* corresponds to solubilized membranes from SK-N-MC and SK-N-MC/H_3 cells analyzed by SDS-PAGE and blotted with anti-H_3R antibody to test the specificity of the antibody. *IP*, immunoprecipitation; *MW*, molecular mass.

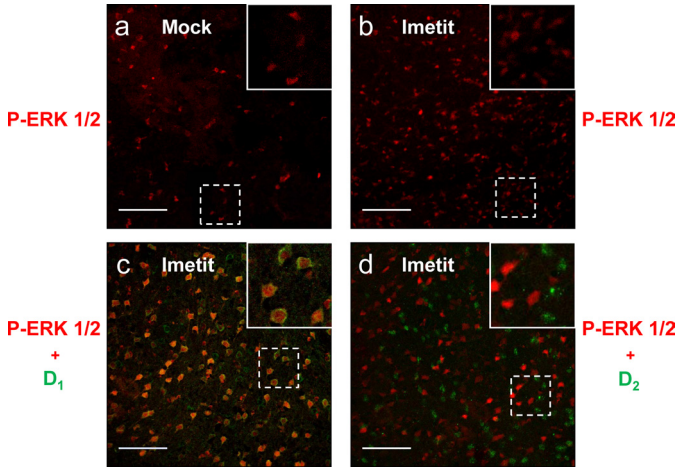

FIGURE 8. **Imetit-induced ERK 1/2 phosphorylation in rat striatal GABAergic neurons.** Confocal microscopy images of coronal sections from striatal slices were treated with medium (*a*) or treated with 1 μM imetit (*b–d*). Slices were labeled with antiphospho-ERK 1/2 antibody (*red*). Labeling (*green*) using an anti-D_1 receptor antibody (*c*), or an anti-D_2 receptor antibody (*d*) is also shown. *Insets* in *c* and *d* are 2× magnification of the indicated parts of the figure. *Scale bars*, 100 μm (*a* and *b*) or 80 μm (*c* and *d*). Representative images of coronal sections are displayed.

A negative cross-talk between striatal D_1R and H_3R has also been described for the adenylyl cyclase-induced signaling pathway, as histamine H_3R activation inhibits D_1R-mediated cAMP accumulation in striatal slices (27). Additional examples of H_3R-mediated responses able to inhibit D_1R-mediated effects are the ability of H_3R agonists to inhibit the effects of D_1R agonists on GABA release in striatal slices (12) and motor activation in reserpinized mice (14). Overall, these results are consistent with an antagonism at the level of adenylyl cyclase between H_3R and D_1R that would not require heteromer formation. In fact, it is known that H_3R and D_1R couple to G_i and G_s, respectively (9, 28–30). Although it is difficult to confirm these results in living animals, studies in transfected cells indicate that D_1R-H_3R heteromers couple to G_i, but not to G_s, to direct histaminergic input toward the MAPK pathway.

Taken together, it appears that histamine and dopamine antagonism mediated by D_1Rs and H_3Rs may rely on balancing ERK activation in GABAergic neurons where D_1R and H_3R are co-expressed and where D_1R-H_3R heteromerization is likely occurring. Heteromers not only allow neurons to differentially "sense" a given neurotransmitter, but they serve to process the different signals impacting them at a given time frame (31, 32). Therefore D_1R-H_3R receptor heteromers would be actively involved in controlling the response of striatal neurons of the direct striatal efferent pathway. The qualitative and quantitative output on ERK 1/2 phosphorylation would largely depend on the concentrations of histamine and dopamine impacting neurons expressing D_1R-H_3R complexes.

Acknowledgments—We acknowledge the technical help obtained from Jasmina Jiménez (Molecular Neurobiology Laboratory, Barcelona University) and Mar Castillo (Neuroscience Institute, Universidad Autónoma de Barcelona).

REFERENCES

1. Albin, R. L., Young, A. B., and Penney, J. B. (1995) *Trends Neurosci.* **18,** 63–64
2. Gerfen, C. R. (2004) in *The Rat Nervous System* (Paxinos G., ed) pp. 445–508, Elsevier Academic Press, Amsterdam
3. Thomas, G. M., and Huganir, R. L. (2004) *Nat. Rev. Neurosci.* **5,** 173–183
4. Santini, E., Alcacer, C., Cacciatore, S., Heiman, M., Hervé, D., Greengard, P., Girault, J. A., Valjent, E., and Fisone, G. (2009) *J. Neurochem.* **108,** 621–633
5. Ryu, J. H., Yanai, K., Iwata, R., Ido, T., and Watanabe, T. (1994) *Neuroreport* **5,** 621–624
6. Pillot, C., Heron, A., Cochois, V., Tardivel-Lacombe, J., Ligneau, X., Schwartz, J. C., and Arrang, J. M. (2002) *Neuroscience* **114,** 173–193
7. Hamill, T. G., Sato, N., Jitsuoka, M., Tokita, S., Sanabria, S., Eng, W., Ryan, C., Krause, S., Takenaga, N., Patel, S., Zeng, Z., Williams, D., Jr., Sur, C., Hargreaves, R., and Burns, H. D. (2009) *Synapse* **63,** 1122–1132
8. Arrang, J. M., Garbarg, M., and Schwartz, J. C. (1983) *Nature* **302,** 832–837
9. Leurs, R., Bakker, R. A., Timmerman, H., and de Esch, I. J. (2005) *Nat. Rev. Drug Discov.* **4,** 107–120
10. Pillot, C., Ortiz, J., Héron, A., Ridray, S., Schwartz, J. C., and Arrang, J. M. (2002) *J. Neurosci.* **22,** 7272–7280
11. García-Ramírez, M., Aceves, J., and Arias-Montaño, J. A. (2004) *Behav. Brain Res.* **154,** 409–415
12. Arias-Montaño, J. A., Floran, B., Garcia, M., Aceves, J., and Young, J. M. (2001) *Br. J. Pharmacol.* **133,** 165–171
13. Hussain, N., Flumerfelt, B. A., and Rajakumar, N. (2002) *Neuroscience* **112,** 427–438
14. Ferrada, C., Ferré, S., Casadó, V., Cortés, A., Justinova, Z., Barnes, C., Canela, E. I., Goldberg, S. R., Leurs, R., Lluis, C., and Franco, R. (2008) *Neuropharmacology* **55,** 190–197
15. Ferrada, C., Moreno, E., Casadó, V., Bongers, G., Cortés, A., Mallol, J., Canela, E. I., Leurs, R., Ferré, S., Lluís, C., and Franco, R. (2009) *Br. J. Pharmacol.* **157,** 64–75
16. Xu, M., Moratalla, R., Gold, L. H., Hiroi, N., Koob, G. F., Graybiel, A. M., and Tonegawa, S. (1994) *Cell* **79,** 729–742
17. Narushima, M., Uchigashima, M., Hashimoto, K., Watanabe, M., and Kano, M. (2006) *Eur. J. Neurosci.* **24,** 2246–2252
18. Hasbi, A., Fan, T., Alijaniaram, M., Nguyen, T., Perreault, M. L., O'Dowd, B. F., and George, S. R. (2009) *Proc. Natl. Acad. Sci. U.S.A.* **106,** 21377–21382
19. Milligan, G., and Bouvier, M. (2005) *FEBS J.* **272,** 2914–2925
20. Pfleger, K. D., and Eidne, K. A. (2006) *Nat. Meth.* **3,** 165–174
21. Franco, R., Casadó, V., Cortés, A., Mallol, J., Ciruela, F., Ferré, S., Lluis, C., and Canela, E. I. (2008) *Br. J. Pharmacol.* **153,** S90-S98
22. Ferré, S., Ciruela, F., Woods, A. S., Lluis, C., and Franco, R. (2007) *Trends Neurosci.* **30,** 440–446
23. Ferré, S., Baler, R., Bouvier, M., Caron, M. G., Devi, L. A., Durroux, T., Fuxe, K., George, S. R., Javitch, J. A., Lohse, M. J., Mackie, K., Milligan, G., Pfleger, K. D., Pin, J. P., Volkow, N. D., Waldhoer, M., Woods, A. S., and Franco, R. (2009) *Nat. Chem. Biol.* **5,** 131–134
24. Casadó, V., Cortés, A., Mallol, J., Pérez-Capote, K., Ferré, S., Lluis, C., Franco, R., and Canela, E. I. (2009) *Pharmacol. Ther.* **124,** 248–257
25. Ellis, J., Pediani, J. D., Canals, M., Milasta, S., and Milligan, G. (2006) *J. Biol. Chem.* **281,** 38812–38824
26. Sánchez-Lemus, E., and Arias-Montaño, J. A. (2004) *Neurosci. Lett.* **364,** 179–184
27. Torrent, A., Moreno-Delgado, D., Gómez-Ramírez, J., Rodríguez-Agudo, D., Rodríguez-Caso, C., Sánchez-Jiménez, F., Blanco, I., and Ortiz, J. (2005) *Mol. Pharmacol.* **67,** 195–203
28. Moreno-Delgado, D., Torrent, A., Gómez-Ramírez, J., de Esch, I., Blanco, I., and Ortiz, J. (2006) *Neuropharmacology* **51,** 517–523
29. Missale, C., Nash, S. R., Robinson, S. W., Jaber, M., and Caron, M. G. (1998) *Physiol. Rev.* **78,** 189–225
30. Rashid, A. J., So, C. H., Kong, M. M., Furtak, T., El-Ghundi, M., Cheng, R., O'Dowd, B. F., and George, S. R. (2007) *Proc. Natl. Acad. Sci. U.S.A.* **104,** 654–659
31. Franco, R. (2009) *Br. J. Pharmacol.* **158,** 23–31
32. Hasbi, A., O'Dowd, B. F., and George, S. R. (2010) *Curr. Op. Pharmacol.* **10,** 93–99